

Welding depth measurement for different mode lasers using optical coherence tomography

Guanming Xie (谢冠明)^{1,2}, Sanhong Wang (王三宏)³, Yueqiang Zhang (张跃强)^{1,2*}, You Li (李由)⁴, Biao Hu (胡彪)^{1,2}, Yu Fu (傅愉)^{1,2}, and Qifeng Yu (于起峰)^{1,2,5}

¹Institute of Intelligent Optical Measurement and Detection, Shenzhen University, Shenzhen 518060, China

²College of Physics and Optoelectronic Engineering, Shenzhen University, Shenzhen 518060, China

³Shenzhen Sincevision Technology Co., Ltd., Shenzhen 518055, China

⁴National Key Laboratory of Human Factors Engineering, China Astronaut Research and Training Center, Beijing 100094, China

⁵College of Aerospace Science and Engineering, National University of Defense Technology, Changsha 410073, China

*Corresponding author: yueqiang.zhang@szu.edu.cn

Received August 28, 2023 | Accepted September 18, 2023 | Posted Online January 18, 2024

Optical coherence tomography (OCT) allows a direct and precise measurement of laser welding depth by coaxially measuring the keyhole depth and can be used for process monitoring and control. When OCT measurement was taken during single-beam laser welding, the keyhole instability of aluminum welding resulted in highly scattered OCT data and complicated the welding depth extraction methods. As a combination of an inner core beam and an outer ring beam, a novel adjustable ring mode (ARM) laser for producing a stable keyhole was applied to the OCT measurement. Different ARM laser power arrangements were conducted on aluminum and copper. The results indicated that the ring beam greatly improved the stability of the core beam-induced keyhole, and smooth welding depth can be extracted from the concentrated OCT data.

Keywords: optical coherence tomography; adjustable ring mode laser; laser welding; welding depth.

DOI: [10.3788/COL202422.011203](https://doi.org/10.3788/COL202422.011203)

1. Introduction

Laser welding has been widely used in industrial manufacturing, and presents unique challenges in the manufacturing of power batteries for electric mobility. A high-precision measurement of laser welding depth is necessary for ensuring sufficient joint strength and avoiding piercing of the battery cells. Compared with the indirect methods relying on photodiodes, cameras, and acoustic monitoring systems^[1-3], optical coherence tomography (OCT) allows a direct and precise measurement of the laser welding depth and shows great promise for process monitoring and control^[4,5].

In laser deep-penetration welding, a vapor capillary named the keyhole appears in the molten pool, and OCT coaxially measures the depth of the keyhole by coupling the measuring beam and processing beam, as shown in Fig. 1. The measurement principle is classified more specifically as spectral-domain OCT (SD-OCT), which is well-established in medical imaging^[6,7]. Light emitted from a superluminescent diode (SLD) is divided by a fiber coupler into sample and reference beams. The two beams are backreflected off the keyhole bottom and the mirror. Both reflected beams are received and analyzed by a spectrometer,

which records the interference spectrogram. A fast Fourier transform (FFT) is performed on the interference spectrogram to resolve the keyhole depth. By deflecting the measuring beam independently of the processing beam using a scanner, OCT can also be used to preprocess or postprocess seam tracking^[8,9].

Generally, a single Gaussian laser beam is used as the process laser owing to its high intensity, which increases the dynamic interaction of laser and material. Compared with steel, aluminum (Al) suffers from high reflectivity and thermal conductivity. In welding Al, the high intensity of the single Gaussian laser beam tends to generate the rapid collapse of the keyhole^[10]. The keyhole dimensions are dynamically changing, which induces noise points from the multiple reflections or the keyhole wall and results in highly scattered OCT data. Boley *et al.*^[11] proposed a statistical filtering method to first exclude the noise points and then extract the welding depth. This method improved the OCT measurement accuracy, but required binning the OCT data into segments and was unsuitable for welding Al. Mittelstadt *et al.*^[12] noticed that histogram evaluation was more suitable for welding Al. However, this required dividing the measuring beam into two subbeams, and significant amount

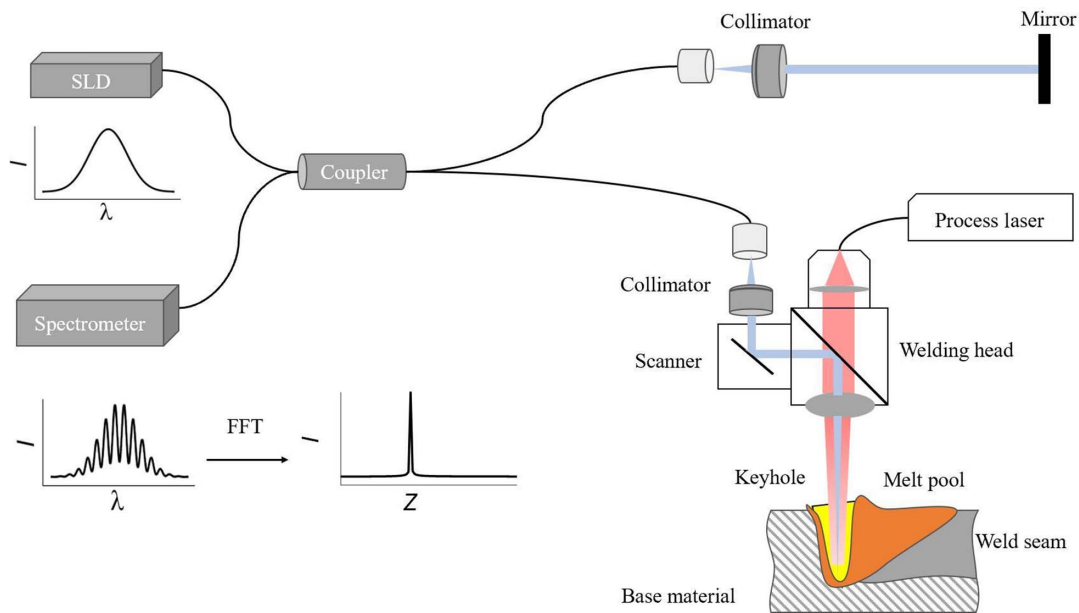


Fig. 1. Schematic of the welding depth measurement system based on SD-OCT.

of the measurement points reflected from the keyhole bottom. In our previous works^[13,14], welding depth measurement using OCT was applied for a single-beam multimode laser. The keyhole instability leads to the highly scattered OCT data for welding Al and complicates the welding depth extraction methods.

To improve the stability of the keyhole, a so-called adjustable ring mode (ARM) laser was introduced. The ARM laser consists of an inner core beam and an outer ring beam, with the capability of dynamically adjusting the power distribution of the two beams. The core Gaussian beam generates the keyhole for sufficiently deep penetration, while the shaped ring beam is expected to stabilize the keyhole by controlling temperature distribution of the melt pool. Maina *et al.*^[15] verified the advantages of ARM laser welding of Al for achieving deeper penetration and better surface quality. Wang *et al.*^[16] investigated the ARM laser welding of Al in terms of welding performance and indicated that the combination of ring beam and core beam greatly improved welding efficiency. Sokolov *et al.*^[17] analyzed the effect of the ARM laser on OCT measurement in overlap welding of aluminum-copper (Al-Cu) and found a reduced keyhole fluctuation, allowing a 50% improvement of the OCT measurement accuracy.

This paper aimed to investigate the welding depth measurement for different mode lasers using OCT. The OCT measurement using single-beam laser welding was compared to ARM laser welding. Different ARM laser power arrangements were conducted on bead-on-plate welding of Al alloy to analyze the influence of the ring beam on OCT measurement. Furthermore, Al alloy and Cu were used for bead-on-plate welding, and overlap welding was conducted to investigate the effect of different materials of ARM laser welding on the OCT measurement.

2. Experimental Setup

Figure 2 illustrates the experimental setup of the welding depth measurement system, which is composed of a laser welding system and an SD-OCT system. Figure 2(a) shows the laser welding system. The welding head had a collimation lens with a focal length of 100 mm and a focusing lens with a focal length of 200 mm. A single-beam multimode laser and an ARM laser were used. Figure 2(b) shows the simulation beam profiles of the multimode laser with 1080 nm wavelength and 6 kW maximum power. The multimode laser was delivered by a fiber with 200 μm core diameter, resulting in 400 μm focus diameter. Figure 2(c) shows the simulation beam profiles of the ARM laser with 1080 nm wavelength and 6 kW maximum power. The ARM laser was configured to output a maximum power of 4 kW in the core beam and a maximum power of 2 kW in the ring beam. Both beams were delivered via a special fiber of 50 μm in core diameter and 150 μm in ring diameter, resulting in a focus diameter of 100 μm in the core and 300 μm in the ring. The power density of the core beam is higher than that of the ring beam, meaning that penetration ability mainly comes from the core beam.

Figure 2(d) shows the SD-OCT system. The 40 mW SLD had an 850 nm central wavelength and 45 nm bandwidth. The emitted light was divided by a 75:25 coupler into the sample and reference beams. The beam in the sample arm, with an output power of 30 mW, was focused into a spot with a diameter of 54 μm . The interference spectrogram was captured by a spectrometer, which had a maximum measuring range of 3 mm and a sampling rate of 80 kHz.

Welding depth measurement using SD-OCT can be applied to laser deep-penetration welding of metal materials (e.g., steel,

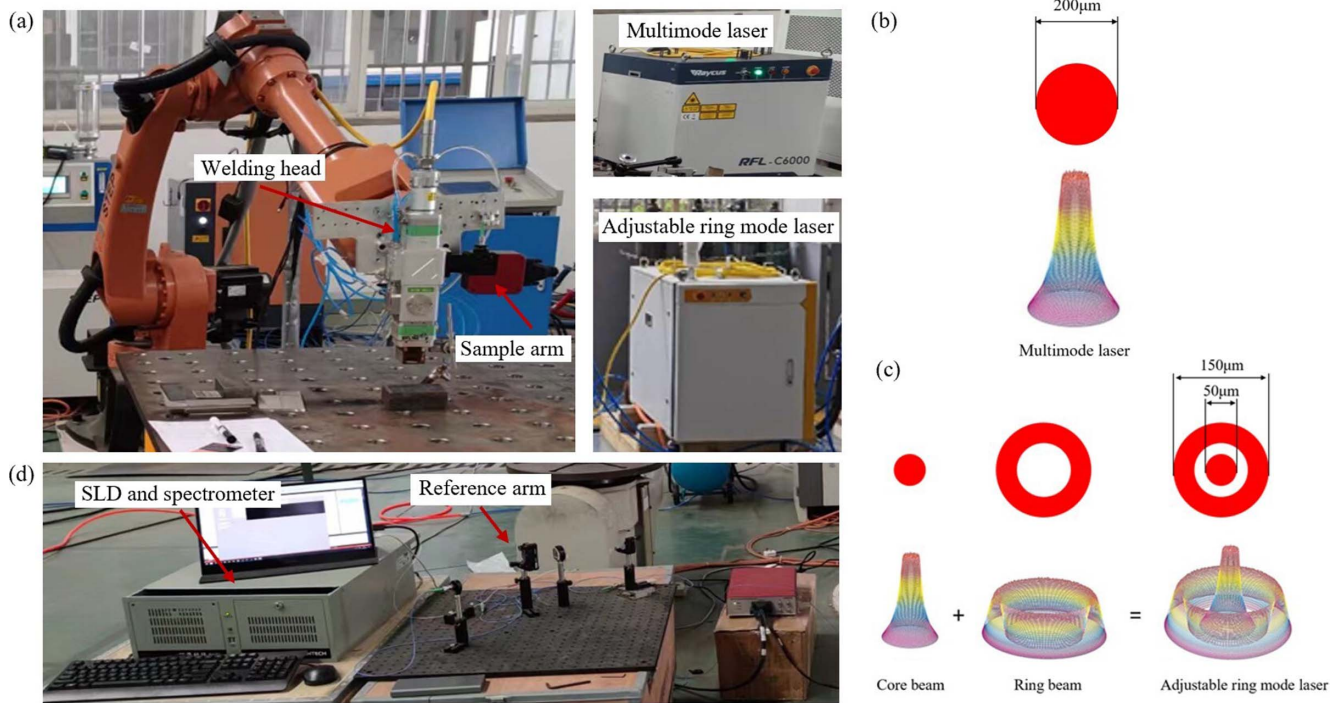


Fig. 2. (a) Laser welding system; (b) beam profiles of the multimode laser; (c) beam profiles of the ARM laser; (d) SD-OCT system.

Table 1. Compositions of Mild Steel Q235, Al Alloy 6061, and Cu T2.

Materials		Chemical Compositions								
Q235	Mn	C	Si	P	Cu	S	Ni	Cr	Fe	
Mass fraction (%)	0.5	0.18	0.25	0.016	0.01	0.018	0.01	0.01	Bal.	
6061	Si	Cu	Fe	Mg	Mn	Cr	Zn	Ni	Al	
Mass fraction (%)	0.6	0.28	0.7	1.0	0.15	0.2	0.25	0.05	Bal.	
T2	P	Ni	Si	Fe	Zn	S	Ag	Pb	Cu	
Mass fraction (%)	0.07	0.02	0.04	0.08	0.09	0.09	0.1	0.005	Bal.	

Al, Cu). Mild steel Q235, Al alloy 6061, and Cu T2 were used. Table 1 shows the chemical compositions. Argon was applied as the shielding gas with a flow rate of 25 L/min.

3. Results and Discussion

The OCT measurement during single-beam laser welding was investigated. The OCT data for bead-on-plate welding of steel and Al were analyzed. Figure 3(a) shows the OCT data for single-beam laser welding of mild steel Q235 with 3 m/min welding speed and 800 W laser power. Since the laser was turned on at 0.03 s and turned off at 0.38 s, the keyhole was measured with a constant welding depth of approximately 0.9 mm from the

concentrated OCT data. The keyhole generated in the steel welding process is stable and rarely collapses.

In contrast with welding steel, there is a major difference in the OCT data for welding Al. Figure 3(b) shows the OCT data for single-beam laser welding of Al alloy 6061 with 3 m/min welding speed and 1750 W laser power. The measurement points are scattered over a very broad range. The keyhole in single-beam laser welding of Al is unstable and collapses frequently. This indicates the greater keyhole instability in the Al welding process than in the steel welding process.

The ARM laser was introduced to generate a stable keyhole in welding Al. To analyze the influence of the ring beam on OCT measurement, pure core and ring/core setups were compared. The process parameters and transverse cross section are shown

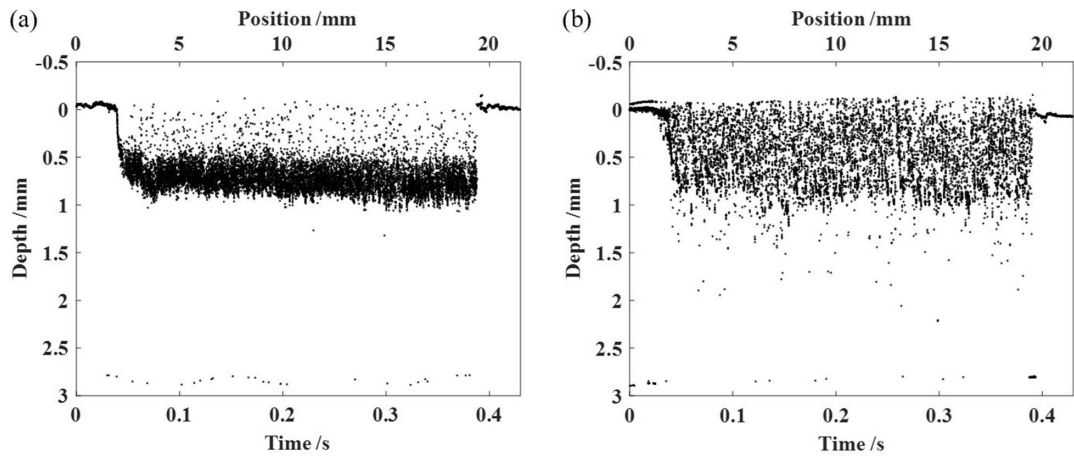


Fig. 3. OCT data for single-beam laser welding of (a) mild steel Q235 with 800 W laser power and (b) Al alloy 6061 with 1750 W laser power at 3 m/min welding speed.

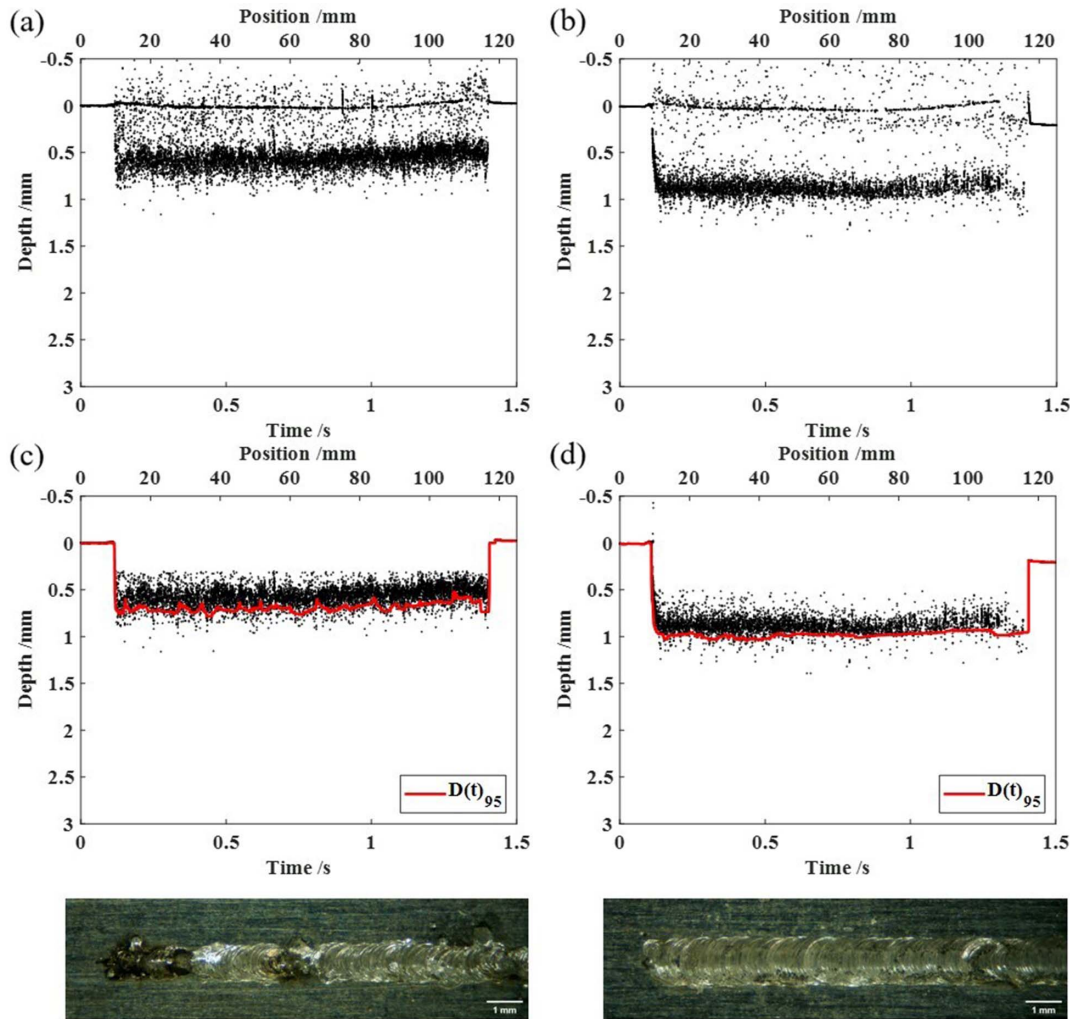
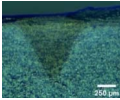
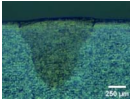


Fig. 4. Top, the OCT data for ARM laser welding of Al alloy 6061 at 5 m/min welding speed with (a), (c) pure core setup and (b), (d) ring/core setup. Bottom, the micrograph of the corresponding seam surface.

Table 2. Process Parameters and Transverse Cross Section.

Setup	Pure Core	Ring/Core
Welding speed	5 m/min	5 m/min
Focus position	0 mm	0 mm
Core power	800 W	800 W
Ring power	0 W	800 W
Actual weld width	0.88 mm	1.09 mm
Actual weld depth	0.77 mm	0.92 mm
Transverse cross section		

in Table 2. The actual weld width and depth in the ring/core setup are greater than those in the pure core setup.

The plots of the OCT data for ARM laser welding of Al alloy 6061 are shown in Fig. 4(a) with the pure core setup and in Fig. 4(b) with the ring/core setup. In both cases, the depths measured in ARM laser welding are more concentrated than those measured in single-beam laser welding. A stable keyhole in the Al welding is generated by the ARM laser. The measurement points at 0 mm during the welding process result from the auto-correlation noise due to the weak multiple reflections within one arm^[18].

The dynamic changes of the keyhole dimensions lead to scattered points in the OCT data, which do not reveal the correct welding depth. To extract the actual welding depth, a well-known nonlinear statistical filtering technique named the

percentile filter was applied, which required the input parameters: percentile p and window length L . According to Ref. [11], it is beneficial to eliminate the noise points before applying the percentile filter. A histogram is the simplest noise removal method. An error of less than 5% can be obtained with a window length above 200 and a percentile between 95 and 98.

Figures 4(c) and 4(d) show the cleaned OCT data after eliminating the noise using the histogram method. The extracted welding depth with $p = 95$ and $L = 400$ is marked by red. The welding depth in the ring/core setup is smoother than that in the pure core setup. The bottom shows the micrographs of the seam surface. The ring/core setup has lower spatter and a better-quality seam surface compared to the pure core setup. This confirms that the ring beam can be used to improve keyhole stability and ensure good surface quality.

To investigate different materials on the OCT measurement, Al and Cu were used. The OCT data are shown in Fig. 5(a) for bead-on-plate welding of Al alloy 6061 with 800 W core power and 800 W ring power and in Fig. 5(b) for bead-on-plate welding of Cu T2 with 1600 W core power and 1600 W ring power. The bottom shows the transverse cross sections and the process parameters. To achieve a constant welding depth of approximately 1 mm, the laser power of welding Cu is twice that of welding Al. The measurement points for Al show smooth welding process, while small-scale fluctuations occur in the Cu welding. The extracted welding depth marked by red in the Al welding is smoother than that in the Cu welding. The distribution difference between Al and Cu can be attributed to the material-dependent geometry of the keyhole because the keyhole of Al welding shows a conical geometry, while Cu welding tends to form a bottle-shaped geometry that generates different reflection patterns^[19].

Dissimilar metal laser welding involves mixing of two materials with different thermal and mechanical properties.

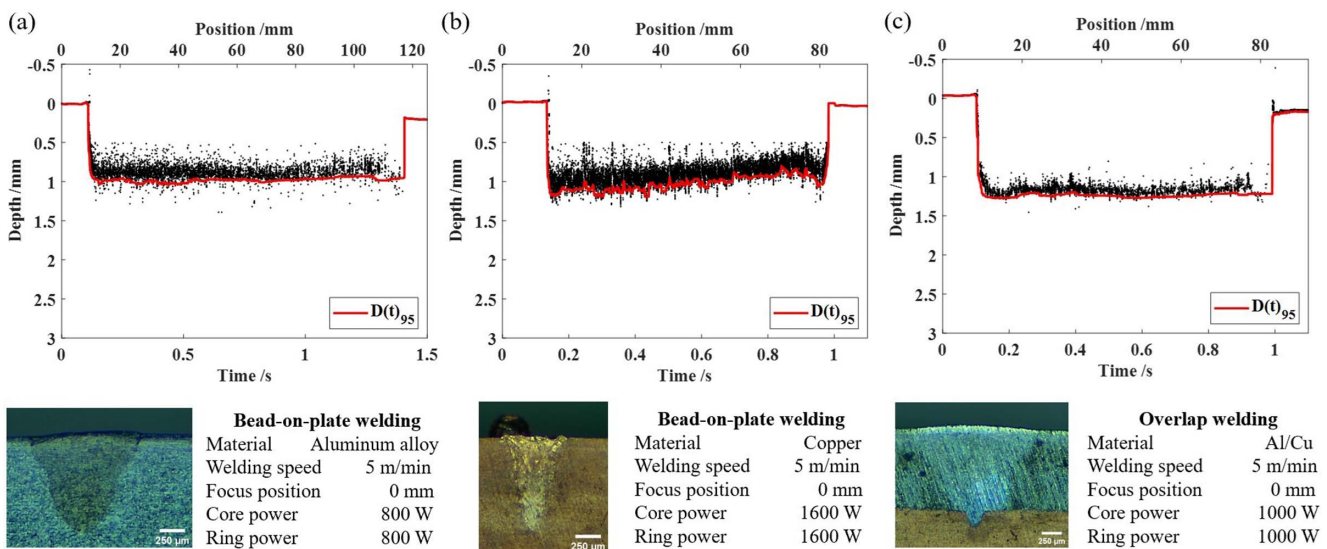


Fig. 5. Top, OCT data for bead-on-plate welding of (a) Al alloy 6061 and (b) Cu T2; (c) OCT data for overlap welding of Al alloy 6061 and Cu T2. Bottom, the corresponding transverse cross section and process parameters.

Figure 5(c) shows the OCT data for overlap welding of Al alloy 6061 and Cu T2 with 1000 W core power and 1000 W ring power. The measurement points during the welding process are scarce but concentrated, which confirms that a stable keyhole occurs in the overlap welding.

4. Conclusion

This work investigated the welding depth measurement for different mode lasers using OCT. For the single-beam welding process with a multimode laser, the results showed highly scattered OCT data for welding Al, which was caused by the keyhole instability. Subsequently, ARM laser was applied to generate a stable keyhole, and OCT measurements with different ARM laser power arrangements were investigated. Concentrated OCT data for welding Al could be obtained, and smoother welding depth could be observed with greater ring power. Furthermore, the influence of the material on the OCT measurement was analyzed. Bead-on-plate welding of Al and Cu was compared, and overlap welding of Al and Cu was conducted. The effectiveness of improving keyhole stability using ARM laser could be confirmed, and the welding depth was determined by OCT.

Future research will focus on the OCT measurement with different ARM laser power arrangements at different welding speeds and the correlation between keyhole status and inner or surface formation.

Acknowledgements

This work was supported by the National Natural Science Foundation of China (No. 12002215), the China Postdoctoral Science Foundation (No. 2022T150437), and the National Key Research and Development Program of China (No. 2019YFC1511102).

References

1. R. Olsson, I. Eriksson, J. Powell, *et al.*, "Challenges to the interpretation of the electromagnetic feedback from laser welding," *Opt. Lasers Eng.* **49**, 188 (2011).

2. C.-H. Kim and D.-C. Ahn, "Coaxial monitoring of keyhole during Yb:YAG laser welding," *Opt. Laser Technol.* **44**, 1874 (2012).
3. H. Gu and W. W. Duley, "A statistical approach to acoustic monitoring of laser welding," *J. Phys. D: Appl. Phys.* **29**, 556 (1996).
4. P. J. Webster, L. G. Wright, Y. Ji, *et al.*, "Automatic laser welding and milling with *in situ* inline coherent imaging," *Opt. Lett.* **39**, 6217 (2014).
5. T. Bautze and M. Kogel-Hollacher, "Keyhole depth is just a distance: the IDM sensor improves laser welding processes," *Laser Tech. J.* **11**, 39 (2014).
6. L. Zhu, Y. Wang, Y. Yuan, *et al.*, "Spectral domain optical coherence tomography with sub-micrometer sensitivity for measurement of central corneal thickness," *Chin. Opt. Lett.* **17**, 041701 (2019).
7. M. Wan, S. Liang, X. Li, *et al.*, "Dual-beam delay-encoded all fiber Doppler optical coherence tomography for *in vivo* measurement of retinal blood flow," *Chin. Opt. Lett.* **20**, 011701 (2022).
8. N. D. Dupriez and C. Truckenbrodt, "OCT for efficient high quality laser welding: high-speed, high-resolution online seam tracking, monitoring and quality control," *Laser Tech. J.* **13**, 37 (2016).
9. C. Stadter, M. Schmoeller, M. Zeitler, *et al.*, "Process control and quality assurance in remote laser beam welding by optical coherence tomography," *J. Laser Appl.* **31**, 022408 (2019).
10. L. Huang, X. Hua, D. Wu, *et al.*, "Numerical study of keyhole instability and porosity formation mechanism in laser welding of aluminum alloy and steel," *J. Mater. Process. Technol.* **252**, 421 (2018).
11. M. Boley, F. Fetzer, R. Weber, *et al.*, "Statistical evaluation method to determine the laser welding depth by optical coherence tomography," *Opt. Lasers Eng.* **119**, 56 (2019).
12. C. Mittelstädt, T. Mattulat, T. Seefeld, *et al.*, "Novel approach for weld depth determination using optical coherence tomography measurement in laser deep penetration welding of aluminum and steel," *J. Laser Appl.* **31**, 022007 (2019).
13. G. Xie, S. Wang, Y. Zhang, *et al.*, "Laser welding depth monitoring method based on optical coherence tomography," *Acta Opt. Sin.* **43**, 1114002 (2023).
14. G. Xie, S. Wang, Y. Zhang, *et al.*, "An efficient method for laser welding depth determination using optical coherence tomography," *Sensors* **23**, 5223 (2023).
15. M. R. Maina, Y. Okamoto, A. Okada, *et al.*, "High surface quality welding of aluminum using adjustable ring-mode fiber laser," *J. Mater. Process. Technol.* **258**, 180 (2018).
16. L. Wang, M. Yao, X. Gao, *et al.*, "Keyhole stability and surface quality during novel adjustable-ring mode laser (ARM) welding of aluminum alloy," *Opt. Laser Technol.* **161**, 109202 (2023).
17. M. Sokolov, P. Franciosa, T. Sun, *et al.*, "Applying optical coherence tomography for weld depth monitoring in remote laser welding of automotive battery tab connectors," *J. Laser Appl.* **33**, 012028 (2021).
18. T. J. Krause, T. R. Allen, and J. M. Fraser, "Self-witnessing coherent imaging for artifact removal and noise filtering," *Opt. Lasers Eng.* **151**, 106936 (2022).
19. M. Schmoeller, C. Stadter, S. Liebl, *et al.*, "Inline weld depth measurement for high brilliance laser beam sources using optical coherence tomography," *J. Laser Appl.* **31**, 022409 (2019).